SIGNAL TRANSDUCTION

Apoptosis propagates through the cytoplasm as trigger waves

Xianrui Cheng[1] and James E. Ferrell Jr.[1,2]*

Apoptosis is an evolutionarily conserved form of programmed cell death critical for development and tissue homeostasis in animals. The apoptotic control network includes several positive feedback loops that may allow apoptosis to spread through the cytoplasm in self-regenerating trigger waves. We tested this possibility in cell-free *Xenopus laevis* egg extracts and observed apoptotic trigger waves with speeds of ~30 micrometers per minute. Fractionation and inhibitor studies implicated multiple feedback loops in generating the waves. Apoptotic oocytes and eggs exhibited surface waves with speeds of ~30 micrometers per minute, which were tightly correlated with caspase activation. Thus, apoptosis spreads through trigger waves in both extracts and intact cells. Our findings show how apoptosis can spread over large distances within a cell and emphasize the general importance of trigger waves in cell signaling.

Xenopus laevis eggs are large cells, ~1.2 mm in diameter, that are naturally arrested in metaphase of meiosis II. The eggs ultimately adopt one of two fates: Either they become fertilized and enter the embryonic cell cycle, or they remain unfertilized and die, usually through apoptosis. Apoptosis is a relatively nonperturbing form of cell death and may allow the frog to resorb old oocytes and to clean up any eggs retained in the body without provoking an inflammatory response (*1*). The powerful biochemical approaches provided by the *Xenopus* system have made *Xenopus* eggs and extracts useful model systems for the study of apoptosis (*2*, *3*).

The unusual size of the *Xenopus* egg raises the question of how an all-or-none, global process such as apoptosis spreads through the cell. One possibility is that apoptosis spreads through the egg by random walk diffusion, ultimately taking over all of the cytoplasm. A second possibility is suggested by the existence of multiple positive and double-negative feedback loops in the regulatory network that controls apoptosis (Fig. 1A). These loops may allow apoptosis to propagate through self-regenerating trigger waves. Trigger waves are propagating fronts of chemical activity that maintain a constant speed and amplitude over large distances. They can arise when bistable biochemical reactions are subject to diffusion or, more generally, when bistability or something akin to bistability (e.g., excitability or relaxation oscillation) is combined with a spatial coupling mechanism (e.g., diffusion or cell-cell communication) (*4*–*6*). Familiar examples include action potentials; calcium waves; and the spread of a fire through a field, a favorable allele through a population, or a meme through the internet. Trigger waves are an important general mechanism for long-range biological communication, and apoptotic trigger waves may allow death signals to spread rapidly and without diminishing in amplitude, even through a cell as large as a frog egg.

To distinguish between diffusive spread and trigger waves in the propagation of apoptotic signals, we used undiluted cell-free extracts from *Xenopus* eggs (*7*). Such extracts can be placed in long tubes (several millimeters) and imaged by video microscopy (*8*, *9*). Over millimeter distances, the distinction between diffusive spread of apoptosis, which would slow down with increasing distance, and trigger waves, which maintain a constant speed and amplitude, should be readily apparent.

We incubated one portion of a cycloheximide-treated interphase cytoplasmic extract with horse cytochrome *c* (2.4 μM) and verified that caspase-3 and/or caspase-7, executioner caspases (*10*) that have similar peptide sequence specificities, became activated (fig. S1). A 10-kDa Texas Red–conjugated dextran was added to the apoptotic extract as a diffusion marker, and the extract was pipetted into a large (560-μm inner diameter) Teflon reservoir. We then took a second portion of the interphase extract, with added sperm chromatin plus a chimeric protein consisting of glutathione *S*-transferase, green fluorescent protein, and a nuclear localization sequence (GST-GFP-NLS) but no cytochrome *c*, and introduced it into a thin (150-μm inner diameter) Teflon tube. The nuclei act as an easily assessed indicator of apoptosis: In nonapoptotic extracts, GST-GFP-NLS concentrates in the nuclei that form from the sperm chromatin, whereas in an apoptotic extract, caspases attack components of the nuclear pore (*11*) and allow the GST-GFP-NLS to leak out and disperse. The tube containing this naïve extract was gently inserted a short distance into the reservoir containing the apoptotic extract, and the two tubes were placed under mineral oil (Fig. 1B). We used time-lapse fluorescence microscopy to determine whether apoptosis spread up the thin tube in a diffusive fashion, with propagation slowing as apoptosis proceeded, or at a constant velocity as expected for trigger waves.

As shown in movie S1 and Fig. 1, B and C, apoptosis progressed up the thin tube at a constant speed of 27 μm/min over a distance of several millimeters. In five independent experiments, apoptosis always propagated linearly, without showing any signs of slowing down or diminishing, and the average speed was 29 ± 2 μm/min (mean ± SD). In contrast, the 10-kDa dye spread only a few hundred micrometers (Fig. 1B), implying that neither simple diffusion nor any unintended mixing could account for the spread of apoptosis.

If the apoptotic signals are propagated by trigger waves, one prediction is that the waves should be self-sustaining; that is, once the activity is established in the thin tube, continued contact with the reservoir of apoptotic extract would not be required. We tested this possibility by inserting the thin tube into the apoptotic reservoir for 20 min and then removing it and monitoring apoptosis. The apoptotic activity propagated from the induction terminus to the distal terminus at a constant speed of 32 μm/min, consistent with a self-sustaining process (fig. S2). This procedure was used for all subsequent experiments because it provided more reliable focusing for the imaging and allowed more tubes to be imaged per experiment.

A second way of detecting apoptosis is with the fluorogenic caspase substrate carboxybenzyl–Asp-Glu-Val-Asp–rhodamine 110 (Z-DEVD-R110) (*12*). This probe is a rhodamine derivative (R110) with two four–amino acid (DEVD) peptides linked to the fluorophore. It is nonfluorescent when the DEVD-fluorophore bonds are intact but becomes strongly fluorescent once they are hydrolyzed by caspase-3 or -7. We added the probe (2 μM) to an extract and initiated apoptosis as before. Fluorescence spread up the tube at a constant speed (in this experiment, 33 μm/min). In eight experiments, the average speed was 30 ± 3 μm/min (mean ± SD) (movie S2 and Fig. 1D). We also added sperm chromatin and GST-mCherry-NLS as well as Z-DEVD-R110 to compare the propagation of the caspase activity wave with the disappearance of the reconstituted nuclei. In this experiment, the disappearance of the nuclei lagged 40 min behind the front of Z-DEVD-R110 fluorescence (Fig. 1E); in four independent experiments, the lag was 35 ± 5 min (mean ± SD). The speeds of the Z-DEVD-R110 and GST-mCherry-NLS waves—the slopes of the dashed lines in Fig. 1E—were indistinguishable.

We sought to understand the mechanistic basis for the trigger waves. The apoptotic control system includes multiple positive feedback loops (Fig. 1A). One positive feedback circuit (designated "caspase loop" in Fig. 1A) involves only cytosolic proteins, including caspases-3, -7, and -9 and XIAP (X-linked inhibitor of apoptosis protein). Another involves the system that regulates the Bak and Bax proteins (the "BH3 protein loop" in Fig. 1A), which, when activated, bring about mitochondrial outer membrane permeabilization (MOMP). One long loop, in which

[1]Department of Chemical and Systems Biology, Stanford University School of Medicine, Stanford, CA 94305-5174, USA. [2]Department of Biochemistry, Stanford University School of Medicine, Stanford, CA 94305-5307, USA.
*Corresponding author. Email: james.ferrell@stanford.edu

cytosolic cytochrome *c* stimulates caspase-3 and -7 activation and caspase activation stimulates cytochrome *c* release (the "MOMP/caspase/BH3 protein loop"), connects the two shorter loops (Fig. 1A). We tested whether the cytosolic components could support trigger waves in the absence of mitochondria and whether the mitochondrial components could support trigger waves in the absence of the activation of caspase-3 and caspase-7.

We fractionated a crude cytoplasmic extract (*2*, *3*) (fig. S3A) and verified by immunoblotting that the resulting cytosol was largely devoid of mitochondria, as indicated by the absence of a mitochondrial marker protein, the voltage-dependent anion channel (fig. S3B). Horse cytochrome *c* (2.4 μM) was added to this cytosolic fraction, and the activity of caspase-3 and/or -7 was assessed by the chromogenic caspase assay. In agreement with previous reports (*3*, *13*), the caspases were briskly activated (Fig. 2A). Thus, mitochondria are not essential for cytochrome *c*–induced activation of executioner caspases in *Xenopus* extracts.

We tested whether the cytosolic extract could support apoptotic trigger waves. Because nuclei cannot be reconstituted in cytosolic extracts, we used the fluorogenic Z-DEVD-R110 probe for this experiment. The fluorescence spread up the tube in a sublinear fashion (movie S3 and Fig. 2E). To see if this spread was consistent with simple random walk diffusion, we identified points along the propagation front with equal fluorescence intensities (fig. S4, A and B) and plotted the distance squared (x^2) versus time (t) (fig. S4C). The x^2-versus-t relationship was linear for at least an hour (fig. S4C), consistent with random walk diffusion. Thus, over this time scale and this distance scale, we found no evidence for a trigger wave.

To further test the role of the mitochondria, we added back purified mitochondria to the cytosolic extract at a 3% volume-to-volume (v/v) ratio, which is approximately physiological [estimated from the volumes we obtained for the various fractions (see fig. S3) and the concentrations used by others in reconstitution studies (*3*)], and again determined whether apoptosis would propagate diffusively or as a trigger wave. As expected, the reconstituted extract activated caspase-3 and/or -7 in response to horse cytochrome *c* (Fig. 2C). Moreover, the reconstitution restored the trigger waves (movie S3 and Fig. 2D). The propagation distance increased linearly with time (Fig. 2D), as it did in crude cytoplasmic extracts

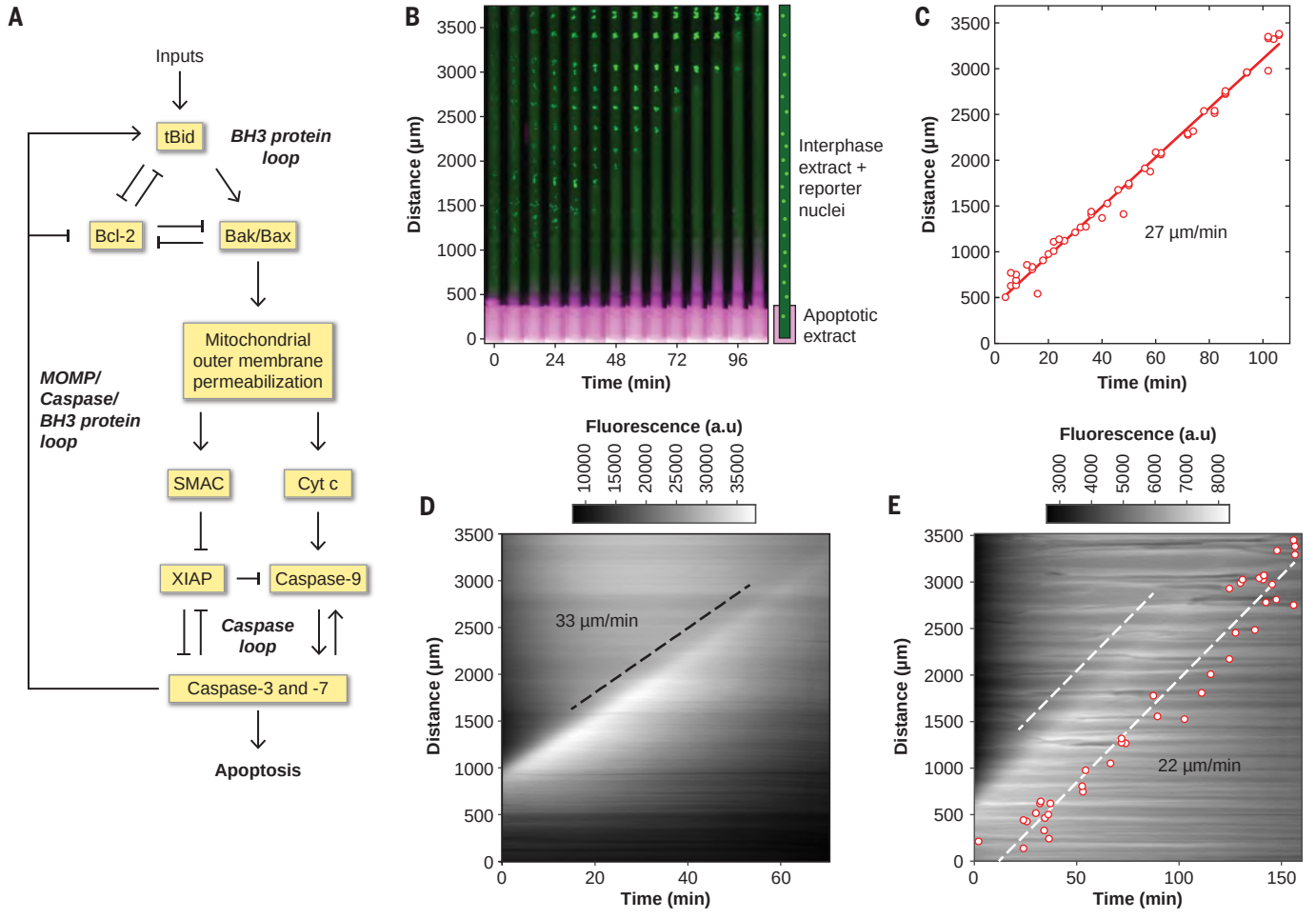

Fig. 1. Apoptosis propagates in interphase-arrested cytoplasmic *X. laevis* egg extracts through trigger waves. (**A**) The control circuit for apoptosis, as conceptualized on the basis of the present study and others' previously published work (*24*–*28*). Cyt c, cytochrome *c*. (**B**) Time-lapse montage of GST-GFP-NLS–filled nuclei (green) in a cytoplasmic extract in a Teflon tube with its lower end in contact with an apoptotic extract reservoir. The extract in the reservoir is marked with 10-kDa dextran–Texas Red dye, shown in magenta. A time-lapse video of this experiment can be found in movie S1. (**C**) Correlation between timing and position of nuclear disappearance for the experiment depicted in (B). The line is a linear least-squares fit to the data. The propagation speed (the slope of the fitted line) is 27 μm/min. (**D**) Kymograph image showing the spatial propagation of caspase-3 and/or caspase-7 activity (indicated by R110 fluorescence) in a crude cytoplasmic extract. The dashed line was manually fitted to the fluorescence front, and it yielded a propagation speed of 33 μm/min. a.u., arbitrary units. (**E**) R110 fluorescence and nuclear disappearance, detected by using GST-mCherry-NLS as a nuclear marker, measured in the same tube. The presence of the nuclei makes the R110 fluorescence less diffuse than it is in (D). One dashed line is manually fitted to the fluorescence front, and the other is a least-squares fit to the nuclear data. The propagation speed was 22 μm/min for both waves.

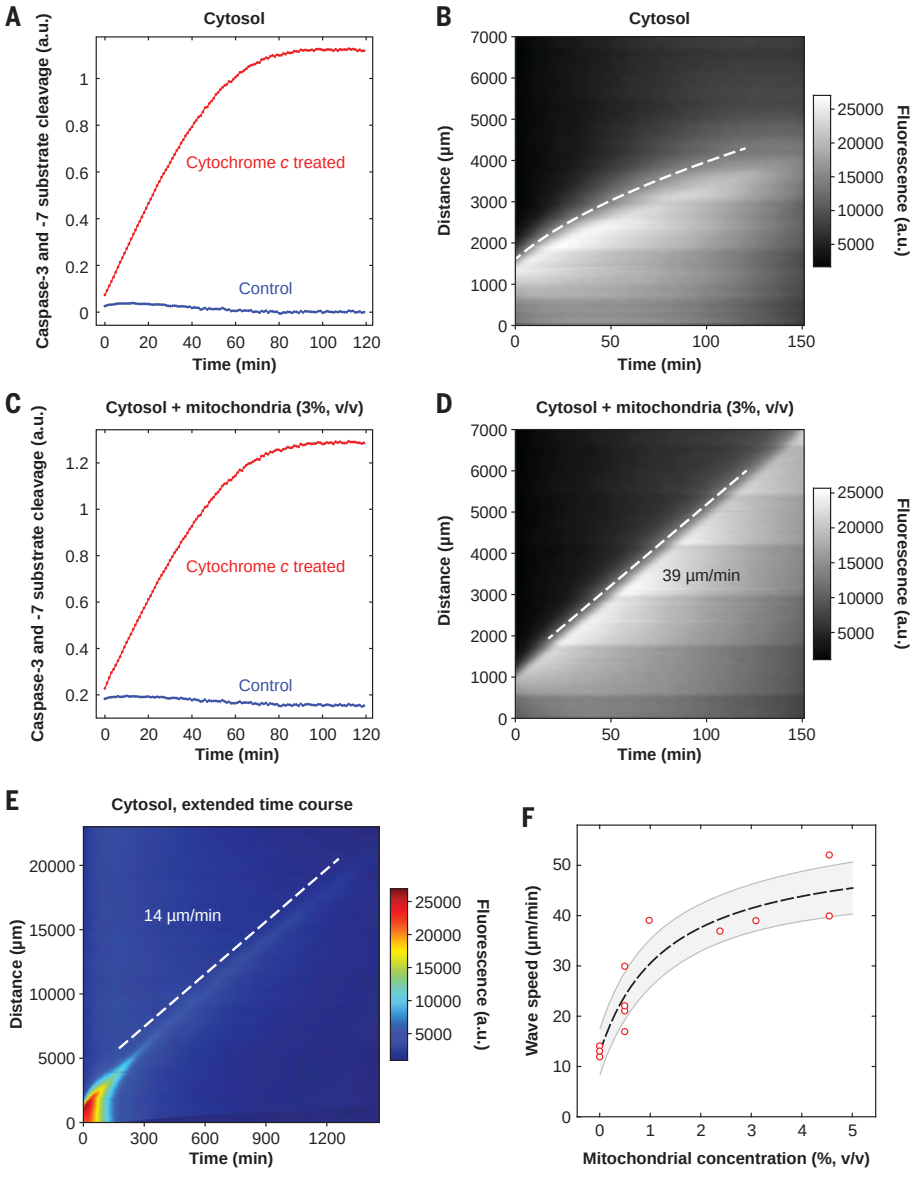

Fig. 2. The speed of the apoptotic trigger wave depends upon the concentration of mitochondria. (**A** and **B**) Cytosolic extract. (A) Activation of caspase-3 and/or caspase-7 as shown by a chromogenic assay. (B) Kymograph image showing diffusive spread of caspase-3 and/or -7 activation, as read out by the Z-DEVD-R110 probe, over the indicated time scale and distance scale. The dashed curve was obtained by defining an equal-fluorescence isocline, replotting the isocline on a distance squared–versus–time plot, carrying out a linear least-squares fit, and then transforming the fitted line for plotting on the original distance-versus-time axes. Further details are provided in fig. S4. (**C** and **D**) Reconstituted extract from the same experiment. (C) Activation of caspase-3 and/or -7. (D) Kymograph image showing trigger wave propagation of caspase activation. (**E**) Slow apoptotic trigger waves detected in cytosolic extracts. This kymograph image represents a cytosolic extract incubated for 24 hours in a 3-cm tube. R110 fluorescence is displayed here on a heat map scale to allow the shape of the wave front to be appreciated both early and late in the time course. (**F**) Wave speed as a function of mitochondrial concentration. Data are from 18 tubes and 8 independent experiments (there are 9 overlapping data points with 0% mitochondria). The dashed line is a Michaelian dose-response curve given by the equation $y = y_0 + y_{max}\frac{x}{K+x}$, where y is the trigger wave speed, x is the mitochondrial concentration, and y_0, y_{max}, and K are parameters determined by fitting the data. The fitted parameters were y_0 = 13.0 ± 1.4 μm/min, y_{max} = 41.3 ± 6.1 μm/min, and K = 1.3 ± 0.6% (means ± SE) and r^2 (coefficient of determination) = 0.98. The region bounded by gray lines represents the SE (68.2% confidence interval) single-prediction confidence band calculated with Mathematica 11.1.1.

(Fig. 1), and propagation occurred at a constant speed of 39 μm/min, somewhat faster than that observed in cytoplasmic extracts. The signal propagated over a long distance (6000 μm) with little loss of amplitude and no loss of speed (Fig. 2D).

Over a distance scale of a millimeter or so, it is easy to distinguish a ~30-μm/min trigger wave from diffusive spread of even a rapidly diffusing small molecule such as R110. However, by the end of the experiment depicted in Fig. 1B, the speed of the caspase-3 wave had fallen to only ~15 μm/min; a trigger wave any slower than that would be outpaced by diffusion over the same distance. Thus, to determine whether trigger waves were abolished or only slowed in cytosolic extracts, we made use of longer tubes (up to 3 cm) and longer time courses (up to 24 hours). Display of R110 fluorescence on a pseudocolor heat map scale made it easier to distinguish the wave front at both early times and late times (Fig. 2E). As was the case in Fig. 2B, the speed of the wave front fell during the first ~120 min, consistent with diffusive propagation, but once the speed reached ~14 μm/min it remained constant for many hours (Fig. 2E). This suggests that purified cytosol is capable of generating apoptotic trigger waves, albeit with a substantially lower speed than that seen in cytoplasm or in cytosol supplemented with mitochondria.

Trigger wave speeds were measured in eight independent experiments with various concentrations of mitochondria (Fig. 2F). From curve fitting, we determined the trigger wave speed to be half maximal at a mitochondrial concentration of 1.3 ± 0.6% (mean ± SE), which is estimated to be ~40% of the physiological mitochondrial concentration in *Xenopus* eggs. Thus, an average concentration of mitochondria is sufficient to generate apoptotic trigger waves of near-maximal speed, and the wave speed would be expected to drop in mitochondrion-poor regions of the cytoplasm.

Apoptosis almost always initiated first at the end of the tube that was dipped in the apoptotic extract (Figs. 1 and 2 and fig. S2). However, in experiments with either cytoplasmic extracts or reconstituted extracts, more than half of the time (in 12 of 22 or 21 of 37 tubes, respectively) a second spontaneous apoptotic wave emerged elsewhere in the tube (movie S4 and fig. S5A). The velocities of the induced and spontaneous trigger waves were indistinguishable (44 μm/min in the example shown in fig. S5A), indicating that they probably represent the same basic phenomenon. The entire tube of extract usually became apoptotic, as assessed by the Z-DEVD-R110 probe, after 2 hours of incubation (fig. S5) and invariably by 4 hours. This global activation of caspase-3 and -7 did not occur in cytosolic extracts (which allowed the extended-time-course experiment depicted in Fig. 2E).

The dependence of the wave speed upon the concentration of mitochondria implies that the BH3-domain proteins that regulate MOMP may function in generating the trigger waves (Fig. 1A). To further test this possibility, we added recombinant GST–Bcl-2 protein to cytoplasmic

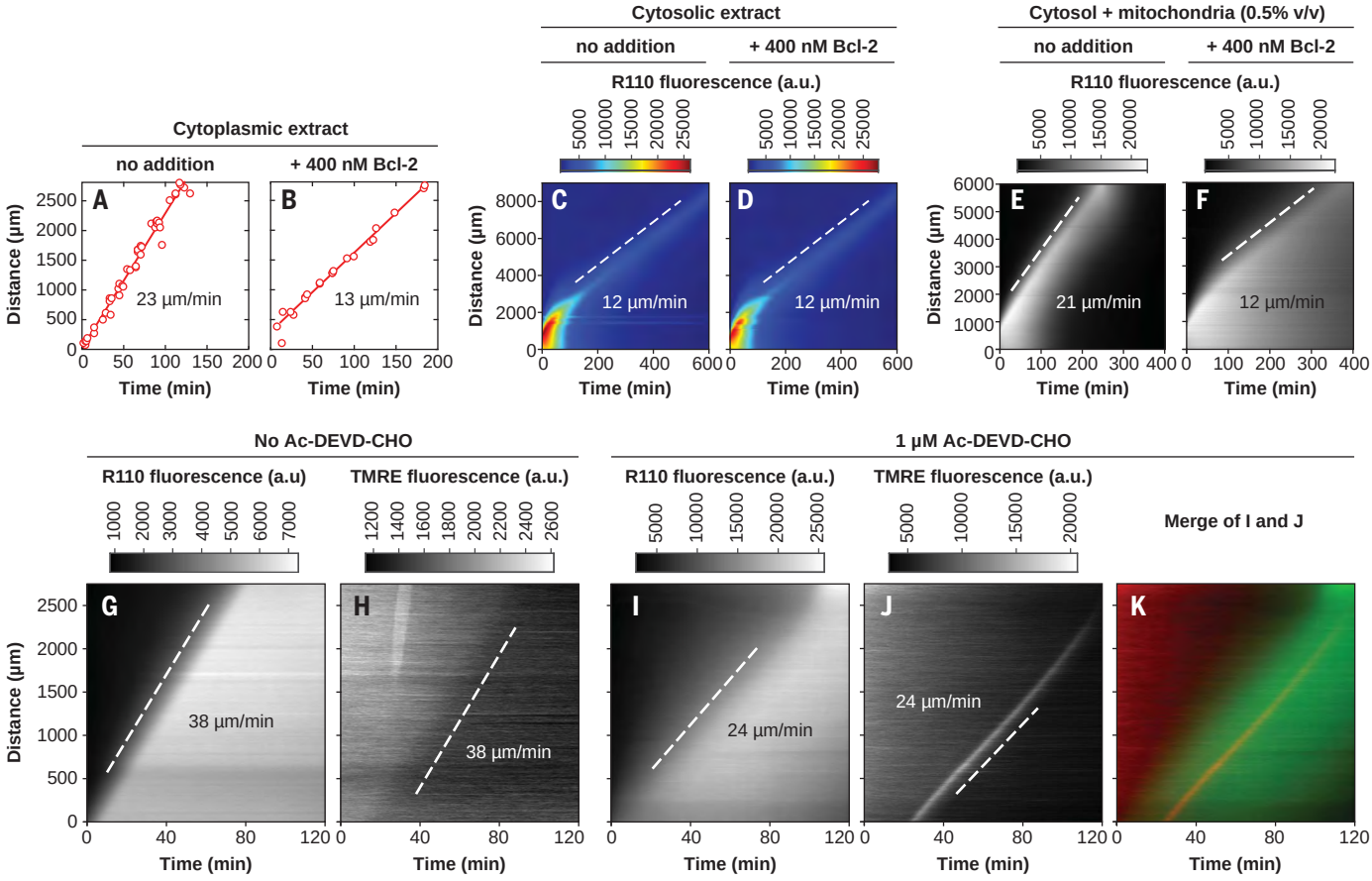

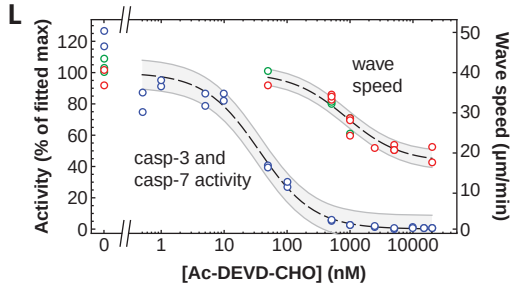

Fig. 3. Both GST–Bcl-2 addition and inhibition of caspase-3 and caspase-7 affect the speed of the trigger waves. (**A** and **B**) GST–Bcl-2 reduces the speed of trigger waves in cytoplasmic extracts. Apoptosis was monitored by the disappearance of reporter nuclei containing GST-mCherry-NLS. (**C** and **D**) GST–Bcl-2 has no effect on the speed of trigger waves in cytosolic extracts. Apoptosis was detected with Z-DEVD-R110, whose fluorescence can be activated by caspase-3 or caspase-7. The pseudocolor heat map scale allows both the initial and final shapes of the wave front to be discerned. (**E** and **F**) GST–Bcl-2 reduces the speed of trigger waves in extracts reconstituted with cytosol and mitochondria (0.5% v/v). (**G** to **K**) Inhibition of caspase-3 and -7 slows trigger waves.
The reporters were Z-DEVD-R110 and the mitochondrial probe TMRE. [(G) and (H)] Cytosolic extract reconstituted with mitochondria (2.4% v/v). [(I) to (K)] A reconstituted extract treated with the caspase inhibitor Ac-DEVD-CHO (1 µM). In experiments with higher concentrations of Ac-DEVD-CHO, a brief (~10 min) period when the TMRE wave appeared to be parabolic rather than linear was observed (fig. S9). (**L**) Inhibition of caspase-3 and -7 activity and slowing of trigger waves as a function of Ac-DEVD-CHO concentration in cytosolic extracts reconstituted with mitochondria (2.4% v/v). Blue data points show caspase activities, measured in extracts diluted 1:20. Green data points indicate wave speeds estimated from Z-DEVD-R110 fluorescence, and red data points indicate wave speeds estimated from TMRE fluorescence. The curves are fits to a Michaelian inhibition function, $y = y_0 + (y_{max} - y_0)\frac{K}{K+x}$, where y is the caspase activity or trigger wave speed, x is the Ac-DEVD-CHO concentration, and y_0, y_{max}, and K are parameters determined by fitting the data. For the caspase activity curve, the fitted parameter values were y_0 = 0.1 ± 2.5, y_{max} = 100 ± 3, and K = 36 ± 8 nM (mean ± SE). For the wave speed curve, the fitted parameter values were y_0 = 17 ± 1 µm/min, y_{max} = 40 ± 1 µm/min, and K = 856 ± 160 nM (mean ± SE). The regions bounded by gray lines represent the SE (68.2% confidence interval) single-prediction confidence bands calculated with Mathematica 11.1.1.

extracts to see whether trigger waves were affected. Bcl-2 is a stoichiometric inhibitor of the pro-apoptotic truncated Bid (tBid) protein and of the pore-forming Bak and Bax proteins, and so the expectation was that GST–Bcl-2 would slow the trigger waves. Adding GST–Bcl-2 decreased the wave speed (Fig. 3, A and B, and movie S5). The maximum effect [at 400 nM added GST–Bcl-2, which compares to the estimated endogenous Bcl-2 concentration of approximately 140 nM (*14*)] was a reduction of the speed to about 13 µm/min, the speed seen in purified cytosol. Added GST–Bcl-2 had no effect on the trigger wave speed in cytosolic extracts (Fig. 3, C and D), which emphasizes that the waves seen in purified cytosol are probably not caused by contaminating mitochondria. GST–Bcl-2 decreased the trigger wave speed in reconstituted (cytosol plus mitochondria) extracts (Fig. 3, E and F), just as it did in cytoplasmic extracts.

If the MOMP–caspase–BH3 protein loop contributed to the generation of trigger waves, inhibition of the executioner caspases would be expected to slow or block the waves (Fig. 1A). To test this, we added the caspase-3 and -7 inhibitor *N*-acetyl–Asp-Glu-Val-Asp–aldehyde (Ac-DEVD-CHO) to the reconstituted extracts. Because high concentrations of the inhibitor make it difficult to monitor trigger waves with the fluorogenic caspase substrate Z-DEVD-R110, we used an additional probe, tetramethylrhodamine ethyl ester (TMRE), a red fluorescent dye that responds to changes in mitochondrial membrane potential.

Nonapoptotic mitochondria accumulate TMRE in their matrices. During apoptosis, the matrix loses TMRE at approximately the time of cytochrome *c* release (*15*, *16*), even in the presence of caspase inhibitors (*17*). We tested TMRE as a reporter of trigger waves by adding 50 nM TMRE to a reconstituted extract, together with Z-DEVD-R110, and looked for evidence of trigger waves in both fluorescence channels. A wave of TMRE loss (and therefore depolarization of mitochondria) could be detected (Fig. 3, G and H). The TMRE wave propagated at the same speed as the caspase trigger wave reported by Z-DEVD-R110 in the same tube (38 μm/min).

We tested whether trigger waves still occurred when caspases-3 and -7 were inhibited. When relatively low (≤ 1 μM) concentrations of the caspase inhibitor Ac-DEVD-CHO were used, there was sufficient residual caspase-3 and/or -7 activity to allow both the Z-DEVD-R110 and TMRE reporters to yield data on trigger wave speed. Both reporters showed that the wave speed decreased as the inhibitor concentration increased (Fig. 3, I to L; fig. S6; and movie S7). In the presence of Ac-DEVD-CHO, a transient increase in TMRE fluorescence occurred at the front of the apoptotic wave, which may result from fluorescence dequenching or transient hyperpolarization and which made the TMRE waves easier to discern (Fig. 3J and movies S6 and S7). At higher concentrations of Ac-DEVD-CHO, the wave speed could be read out only with the TMRE reporter, and it leveled off at ~15 μm/min (Fig. 3L).

These experiments implicate caspase-3 and/or -7 as well as Bcl-2 in the regulation of the apoptotic trigger waves. The experiments also show that the trigger waves are relatively robust; they are still present, though with reduced speeds, in extracts depleted of mitochondria or treated with maximal doses of GST–Bcl-2 or Ac-DEVD-CHO. However, the addition of Ac-DEVD-CHO to cytosolic extracts did completely eliminate trigger waves (fig. S7). Thus, the cytosolic caspase feedback loop (Fig. 1A) appears to mediate the (slow) apoptotic trigger waves seen in purified cytosolic extracts (Figs. 2E and 3C).

To determine whether apoptotic trigger waves occur in intact oocytes and eggs, we imaged oocytes incubated with TMRE or Z-DEVD-R110 and looked for evidence of a wave of fluorescence. However, the opacity of the cells made it difficult to obtain satisfactory imaging data. Nevertheless, we noticed that when oocytes were injected with cytochrome *c*, a wave of changes in the oocyte's natural pigmentation systematically spread from the site of injection to the opposite pole. One particularly notable example of such a wave is shown in montage form in Fig. 4A, as a kymograph image in Fig. 4B, and in video form in movie S8; two more-subtle examples are shown in movie S9. The surface waves propagated at an apparent speed of ~30 μm/min, similar to the wave speeds seen in apoptotic extracts. Control oocytes injected with Texas Red–dextran in water did not exhibit these surface waves. These findings indicate that apoptotic trigger waves can be produced in oocytes.

To test whether eggs might naturally exhibit a similar surface wave at the end of their lifetimes, we incubated eggs with egg-laying buffer at room temperature, conditions that typically lead to apoptosis by 12 to 24 hours. During this same time period, a surface wave often appeared, originating near the vegetal pole and propagating toward the animal pole, with a typical apparent speed of ~30 μm/min (Fig. 4, C and D, and movie S10). This wave was followed by further pigment changes over the next several hours—expansion and then contraction of a white dot at the animal pole (fig. S8).

To see whether the surface wave correlated with caspase activation, we harvested and lysed individual eggs just after they underwent such a wave. Every egg that showed a wave had increased caspase activity (Fig. 4, E and F, red symbols). We also collected eggs during the same time period that had not displayed a wave. None of these eggs had increased caspase activity (Fig. 4, E and F, blue symbols). These findings support the idea that spontaneous apoptosis typically initiates near the vegetal pole of the egg and propagates outward and upward from there as a ~30-μm/min trigger wave.

Our results indicate that apoptosis propagates through cytoplasmic *X. laevis* extracts via trigger waves (Fig. 1). The speed of the apoptotic trigger waves depends upon the concentration of mitochondria, although both cytosolic extracts and GST–Bcl-2–treated cytoplasmic extracts can support slower (~13 μm/min) waves (Figs. 2 and 3). Inhibiting caspase-3 and caspase-7 also slowed but did not abolish the waves. These findings show that the phenomenon is highly robust and must involve multiple interlinked bistable systems. We also found evidence for apoptotic waves in cytochrome *c*–injected oocytes and in spontaneously dying eggs, demonstrating that the trigger waves are not an artifact of the extract system.

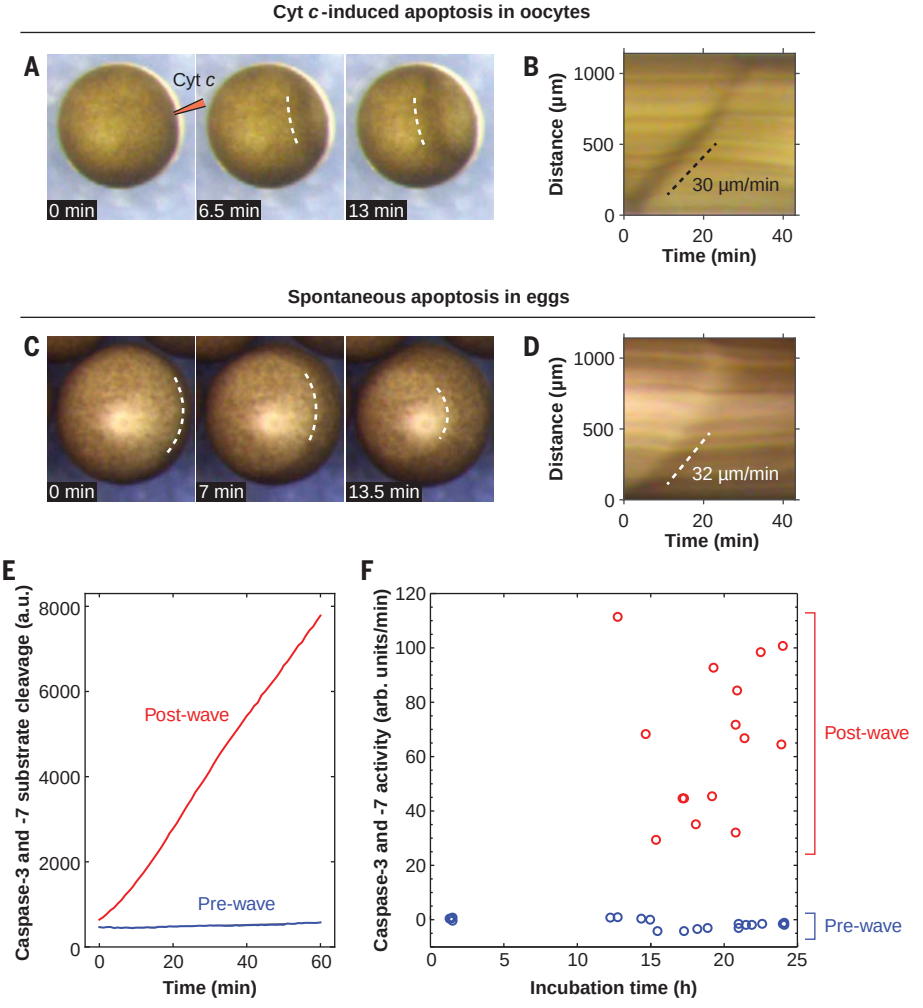

Fig. 4. Apoptotic trigger waves in intact oocytes and eggs. (**A** and **B**) Injection of immature stage VI oocytes with cytochrome *c* (10 nl of 1-mg/ml cytochrome *c*) causes a wave of pigmentation changes to spread from the injection site to the opposite side of the oocyte. (A) Surface wave example shown in montage form. Dashed lines highlight the progress of the wave. (B) Kymograph image. Two other examples of these waves are shown in movie S9. (**C** and **D**) Surface waves occur in spontaneously dying eggs. (C) Surface wave example shown in montage form. (D) Kymograph image. (**E**) Caspase-3 and/or caspase-7 assays for one prewave and one postwave egg. (**F**) Caspase-3 and/or -7 activities for eggs pre- and postwave. The data are from 19 prewave eggs and 15 postwave eggs.

Imaging studies on mammalian cell lines (*18*–*20*), cardiac myotubes (*21*, *22*), and syncytial human trophoblasts (*23*) have shown that apoptosis typically initiates at a single discrete focus or a small number of discrete foci and then spreads rapidly throughout the cell, and in some of these studies the propagation velocities appeared to be constant over distances of ~100 μm (*18*, *19*, *21*, *22*). Although it can be difficult to distinguish between trigger waves and diffusive spread over such short distances, particularly in cells with irregular geometries and inhomogeneous cytoplasm, it seems likely that apoptotic trigger waves occur in many cell types.

There is a close analogy between the mechanisms underpinning the apoptotic trigger waves observed in this study and calcium waves. Calcium waves arise from calcium-induced calcium release from the endoplasmic reticulum; apoptotic waves involve cytochrome *c*–induced release of cytochrome *c* from the mitochondria. The particular proteins, storage organelles, and time scales are different, but the basic logic is the same.

The ingredients needed for generating a trigger wave are simple; they include a spatial coupling mechanism (such as diffusion or intercellular communication) and positive feedback (*6*). Positive feedback is commonplace in signal transduction, from cell fate induction to biological oscillations to prion formation. And whenever positive feedback is present, there is a possibility of trigger waves, allowing signals to propagate quickly over large distances without diminishing in strength or speed. We suspect that many other examples of trigger waves exist in intra- and intercellular communication.

REFERENCES AND NOTES

1. S. Iguchi, T. Iwasaki, Y. Fukami, A. A. Tokmakov, *BMC Cell Biol.* **14**, 11 (2013).
2. D. D. Newmeyer, D. M. Farschon, J. C. Reed, *Cell* **79**, 353–364 (1994).
3. P. Deming, S. Kornbluth, *Methods Mol. Biol.* **322**, 379–393 (2006).
4. J. J. Tyson, J. P. Keener, *Physica D* **32**, 327–361 (1988).
5. A. T. Winfree, *Faraday Symp. Chem. Soc.* **9**, 38–46 (1974).
6. L. Gelens, G. A. Anderson, J. E. Ferrell Jr., *Mol. Biol. Cell* **25**, 3486–3493 (2014).
7. A. W. Murray, *Methods Cell Biol.* **36**, 581–605 (1991).
8. J. B. Chang, J. E. Ferrell Jr., *Nature* **500**, 603–607 (2013).
9. J. B. Chang, J. E. Ferrell Jr., *Cold Spring Harb. Protoc.* 10.1101/pdb.prot097212 (2018).
10. S. W. Tait, D. R. Green, *Nat. Rev. Mol. Cell Biol.* **11**, 621–632 (2010).
11. E. Ferrando-May, *Cell Death Differ.* **12**, 1263–1276 (2005).
12. J. Liu *et al.*, *Bioorg. Med. Chem. Lett.* **9**, 3231–3236 (1999).
13. H. Zou, Y. Li, X. Liu, X. Wang, *J. Biol. Chem.* **274**, 11549–11556 (1999).
14. M. Wühr *et al.*, *Curr. Biol.* **24**, 1467–1475 (2014).
15. J. C. Goldstein, N. J. Waterhouse, P. Juin, G. I. Evan, D. R. Green, *Nat. Cell Biol.* **2**, 156–162 (2000).
16. M. Rehm, H. Düssmann, J. H. Prehn, *J. Cell Biol.* **162**, 1031–1043 (2003).
17. N. J. Waterhouse *et al.*, *J. Cell Biol.* **153**, 319–328 (2001).
18. L. Lartigue *et al.*, *J. Cell Sci.* **121**, 3515–3523 (2008).
19. P. D. Bhola, A. L. Mattheyses, S. M. Simon, *Biophys. J.* **97**, 2222–2231 (2009).
20. M. Rehm *et al.*, *Cell Death Differ.* **16**, 613–623 (2009).
21. P. Pacher, G. Hajnóczky, *EMBO J.* **20**, 4107–4121 (2001).
22. C. Garcia-Perez *et al.*, *Proc. Natl. Acad. Sci. U.S.A.* **109**, 4497–4502 (2012).
23. M. S. Longtine, A. Barton, B. Chen, D. M. Nelson, *Placenta* **33**, 971–976 (2012).
24. E. H. Cheng *et al.*, *Science* **278**, 1966–1968 (1997).
25. E. A. Slee, S. A. Keogh, S. J. Martin, *Cell Death Differ.* **7**, 556–565 (2000).
26. J. G. Albeck, J. M. Burke, S. L. Spencer, D. A. Lauffenburger, P. K. Sorger, *PLOS Biol.* **6**, e299 (2008).
27. S. Legewie, N. Blüthgen, H. Herzel, *PLOS Comput. Biol.* **2**, e120 (2006).
28. T. Zhang, P. Brazhnik, J. J. Tyson, *Biophys. J.* **97**, 415–434 (2009).

ACKNOWLEDGMENTS

We thank the members of J. Chen's and D. Jarosz's labs for sharing their microscopes, H. Funabiki and M. Dasso for providing the GST-GFP-NLS construct, and J. Kamenz and the rest of the Ferrell lab for helpful discussions and comments on the manuscript. **Funding:** This work was supported by grants from the National Institutes of Health (R01 GM110564 and P50 GM107615). **Author contributions:** X.C. and J.E.F. jointly designed the studies, carried out the computations, made the figures, and wrote the paper. X.C. carried out the experiments. **Competing interests:** None declared. **Data and materials availability:** All data needed to evaluate the conclusions in the paper are present in the paper or the supplementary materials.

SUPPLEMENTARY MATERIALS

www.sciencemag.org/content/361/6402/607/suppl/DC1
Materials and Methods
Figs. S1 to S9
Movies S1 to S10

21 June 2016; resubmitted 15 December 2017
Accepted 3 July 2018
10.1126/science.aah4065